Korea-Australia Rheology Journal, Vol.26, No.3, pp.311-318 (August 2014) www.springer.com/13367
DOI: 10.1007/s13367-014-0035-z

Effects of mixing protocol and mixing time on viscoelasticity of compatibilized PP/PS blends

Reza Salehiyan[1], Woo Jin Choi[2], Jun Hyup Lee[3] and Kyu Hyun[1,*]

[1]*School of Chemical and Biomolecular Engineering, Pusan National University, Busan 609-735, Republic of Korea*
[2]*Chemical Materials, Solution Center, Korea Research Institute of Chemical Technology, Daejeon 305-600, Republic of Korea*
[3]*Department of Chemical Engineering, Myongji University, Yongin, Gyeonggi-do 449-728, Republic of Korea*

(Received January 27, 2014; final revision June 2, 2014; accepted June 4, 2014)

Linear and non-linear viscoelastic properties of Polypropylene (PP)/Polystyrene (PS) blends with organoclay (C20A) as a compatibilizer were investigated using dynamic oscillatory measurement, *i.e.*, small amplitude oscillatory shear (SAOS) and large amplitude oscillatory shear (LAOS) tests. Four different mixing protocols were applied to probe the effect of mixing sequence on rheological properties. Moreover, each protocol was conducted at three mixing times, *i.e.*, 1, 3, and 8 min, to investigate the effect of mixing time on final rheological properties. Final results revealed that mixing time had no significant effect on either the viscoelastic response of the simultaneously mixed blends or the PP+C20A/PS (PP and C20A mixed for 30 seconds and then PS added) blend. On the other hand, rheological properties of the PS+C20A/PP (PS and C20A mixed for 30 seconds and then PP added) blend significantly increased upon 1 min of total mixing time, whereas 3 and 8 min of mixing demonstrated almost the same results as their other blended counterparts. TEM pictures revealed migration of C20A particles from PS phase towards the interface with increasing mixing time.

***Keywords*:** linear and non-linear viscoelastic properties, PP/PS/C20A blends, mixing protocol, mixing time

1. Introduction

During the past few decades, many researchers have focused on the morphological evolution of compatibilized blends since morphology has a great impact on their final properties (Harrats, 2010). However, most polymers are thermodynamically immiscible, as droplets of the minor phase are dispersed in a continuous phase of the matrix. Compatibilizers can be used as emulsifiers to improve compatibilities in particular blends when carefully designed, owing to their interfacial activity (Fayt *et al.*, 1981; Utracki and Summut, 1988; Utracki, 1991; Brahimi *et al.*, 1991). Recently, inorganic fillers have been used as alternative compatibilizers due to their unique enhancement of mechanical, thermal, and barrier properties (Wang *et al.*, 2003; Ray *et al.*, 2004; Hong *et al.*, 2007; Huitric *et al.*, 2009; Cho *et al.*, 2011; Labaume *et al.*, 2013; Salehiyan *et al.*, 2013; Salehiyan and Hyun, 2013). Rheological analysis has been extensively used in order to investigate the morphological evolution and internal structures of compatibilized blends (Gleinser *et al.*, 1994; Asthana and Jayaraman, 1999; Iza *et al.*, 2001; Van Puyvelde *et al.*, 2001; Raghu *et al.*, 2003; Van Hemelrijck *et al.*, 2003; Macaubas *et al.*, 2005; Elias *et al.*, 2007; 2008). It has also been reported that processing conditions as well as other factors such as concentration, blend composition, and particle orientation throughout the blend are key factors affecting morphological development (Wang *et al.*, 2003; Vermant *et al.*, 2004; Mederic *et al.*, 2005; Lertwimolnun and Vergnes, 2006; Li *et al.*, 2007; Elias *et al.*, 2007; 2008a; 2008b; Hong *et al.*, 2008; Cho *et al.* 2011; Zonder *et al.*, 2011).

Wang *et al.* (2003) previously showed that increasing mixing time of (70/30) PP/PS/organo-modified Montmorillonite (OMMT) blends effectively induces domain size reductions along with a more uniform distribution. Mederic *et al.* (2005) studied the effect of increasing rotational speed of the blades on PA12 (polyamide12)/C30B (clay, 2.5%) nanocomposites prepared at a fixed mixing time of 6 min. The peak associated with d-basal spacing of the C30B clay galleries gradually disapeared as rotor speed increased, indicating exfoliation of the clay due to shear-induced diffusion of PA12 chains into the clay galleries. Moreover, the storage modulus G'(ω) of the PA12/C30B nanocomposite mixed at 100 rpm was three times higher than that of the nanocomposite mixed at 32 rpm. This increase in storage modulus G'(ω) of the nanocomposites with increasing rotor speed can be explained by the degree of exfoliation, which is consistent with x-ray diffraction patterns. Li *et al.* (2007) revealed the compatibilization effect of styrene-butadiene-styrene (SBS) copolymer on a (20/80) PP/PS blend with different mixing times. Their results verified the ability of SBS to reduce drop size as well as increase complex viscosity. However, morphological observations suggested that this size reduction occurred within the first 2 min of mixing. Elias *et al.* (2007) investigated the effects of two different hyrdophilic and hyrdrophobic fumed silica on a (70/30) PP/PS blend.

*Corresponding author: kyuhyun@pusan.ac.kr

Their results showed that hydrophilic fumed silica was located inside PS drops while hydrophobic ones remained in PP phase or at the interface. Both resulted in a smaller drop size regardless of suppressed coalescence or interfacial tension reduction mechanisms. However, silica particles pre-mixed with PP and then blended with PS migrated towards PS phase. Therefore, the linear rheological properties and final morphologies of the blends are not dependent on the nature or localization of the silica particles. Similarly, Vermant *et al.* (2004) reported that morphological developments of (70/30) polydimethylsiloxane/polyisobutylene/silica (PDMS/PIB/silica) blends are independent of mixing protocols. Further, Elias *et al.* (2008a) studied the effects of hydrophilic and hydrophobic silica particles on (80/20) polypropylene/ethylene-co-vinyl acetate (PP/EVA) blends. In the case of simultaneously mixed blends, hydrophilic silica was located inside of the EVA-dispersed droplets while hydrophobic silica was accommodated at the interface. On the other hand, pre-mixed silica with PP and then blended with EVA was found to be located with the EVA droplets close to the interface. This result indicated that silica particles migrated towards EVA phase for a more favorable interaction. Therefore, although morphological developments do not depend on the nature of the silica, effective interfacial tension decreases when silica particles are located in the dispersed phase.

Alternatively, the effects of shear stress on the localization of organoclays within a PBT/PS blend were examined by Hong *et al.* (2008). They found that clay particles never migrated towards PS phase and always remained in PBT phase at all shear rates regardless of the mixing protocol. This result suggests that chemical affinity between the clay and multiple phases is the critical factor for inducing migration of the clays and not the flow itself. Cho *et al.* (2011) observed that C20A (clay) particles migrated towards PS phase in a PP/PS blend as mixing time increased. They concluded that the most striking improvement of linear rheological properties occurs within the early stages of mixing. Later on, it was revealed that the location of carbon nanotubes (CNTs) has a remarkable influence on the morphologies, rheological properties, and electrical behaviors of polyamide12/high density polyethyelene (PA12/PE/CNT) blends (Zonder *et al.*, 2011). Finer morphology was obtained when CNTs were premixed with PE phase, resulting in solid-like behavior in the case of PE+CNT/PA. These improvements were observed despite CNTs supposedly having better affinity towards PA phase. This can be explained by enhanced compatibility between PA and PE phases, and CNTs were found to be located at the interface as a result of migration when pre-mixed with PE. More interestingly, CNTs at the interface increased conductivity of the blend by showing reduced resistivity when pre-mixed with PE.

The literature shows that orientation of the fillers within a blend critically determines its final properties. Processing conditions such as mixing protocol and mixing time can play key roles in determining the final orientation of the fillers by inducing migration. In the present work, the effects of mixing protocol and mixing time on PP/PS/C20A blends were studied by examining linear and non-linear rheological properties from small amplitude oscillatory shear (SAOS) and large amplitude oscillatory shear (LAOS) tests. Most previous works have focused on linear rheological properties from SAOS tests in order to study the correlation between rheology and morphology evolution. Lim et al. (2013) and Salehiyan and Hyun (2013) reported that the non-linear rheological properties from LAOS tests are very sensitive to polymer morphology. In this study, both linear rheological properties from SAOS tests and non-linear rheological properties from LAOS tests with FT-Rheology were investigated.

2. Experimental

2.1. Materials

The polypropylene (PP), (MI = 6.0 g/min at 230°C, grade HP562T), used in this study was obtained from PolyMirae Company Ltd. The polystyrene (PS), (MI = 1.760 g/min at 200°C, grade HF2680), was provided from Samsung Cheil Industries Inc. The organoclay, Cloisite20A (C20A), was purchased from Southern Clay Products Inc. Cloisite20A is a dimethyl-hydrogenated tallow ammonium-modified montmorillonite with density of 1.77 g/cm^3.

2.2. Blend preparations

All samples were dried in a vacuum oven at 80°C for 12 hours prior to compounding. C20A was kept in a convection oven at 100°C for extra moisture removal. The samples were mixed using a Haake mixer (Thermo Fisher Scientific Inc.) at 50 rpm and 200°C. The blend composition was 80/20/5 wt% in which PP is the matrix and PS is the dispersed phase. After melt blending, pellets were compressed and molded into disks with a diameter of 25 mm and thickness of 1 mm at 200°C. In order to observe the effects of mixing time evolutions, the amount of C20A was fixed at 5 wt%, and all protocols were conducted at three different mixing times of 1, 3, and 8 min. Details of the mixing protocols are shown as follows:

1) P_1 = Simultaneous mixing: All three components were mixed at the same time
2) P_2 = PP+C20A/PS: PP and C20A premixed for 30 seconds, and then PS added
3) P_3 = PS+C20A/PP: PS and C20A premixed for 30 seconds, and then PP added
4) P_4 = PP+PS/C20A: PP and PS premixed for 30 seconds, and then C20A added

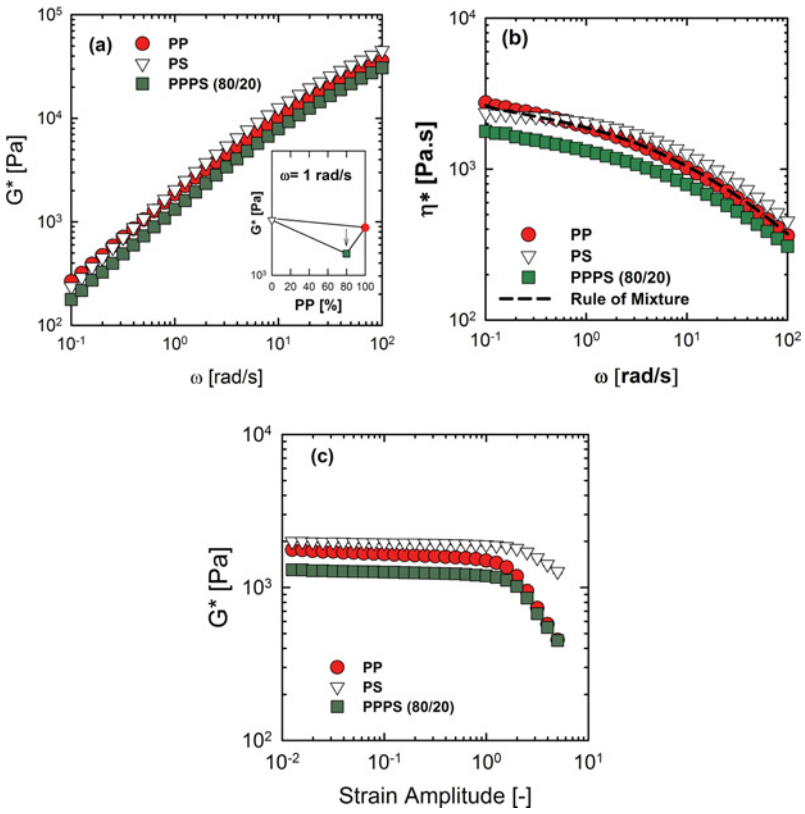

Fig. 1. (Color online) (a) Complex moduli G*(ω) and (b) Complex viscosity $\eta^*(\omega)$ for the PP, PS, and PP/PS (80/20) blends as a function of frequency from 0.1 to 100 rad/s at a fixed strain amplitude of 0.05 and temperature of 200°C. (c) Complex moduli G*(γ_0) for the PP, PS, and (80/20) PP/PS blends as a function of strain amplitude from 0.01 to 5 at a fixed frequency of 1 rad/s and temperature of 200°C. For better comparison, all compounds were mixed in a fixed time of 5 min at 50 rpm.

2.3. Rheological measurements

Two strain controlled rheometers RDA II (Rheometrics Inc.) and AERS-G2 (TA Instruments) with 25 mm parallel plate geometries were used to carry out rheological measurements. Frequency sweep tests were used to obtain linear rheological responses under small amplitude oscillatory shear (SAOS) flow. Strain amplitudes were kept small enough (γ_0 = 0.05) to ensure they were within linear viscoelastic regime. Non-linear rheological properties were obtained through strain sweep tests under large amplitude oscillatory shear (LAOS) flows with increasing strain amplitude from γ_0 = 0.01 to 5 at a fixed frequency of 1 rad/s.

FT-Rheology was used for quantification of the non-linear stress responses of polymer blends. FT-Rheology decomposes the stress data in time domains into the intensities in frequency domains. Eqn. (1) and (2) describe the mathematical decomposition process (Wilhelm *et al.*, 1998; 1999; 2000; Hyun *et al.*, 2012).

$$\sigma(t) = \sigma_1 \sin(\omega t + \delta_1) + \sigma_3 \sin(3\omega t + \delta_3) + \sigma_5 \sin(5\omega t + \delta_5) + \ldots , \quad (1)$$

$$\sigma(t) \propto I_1 \sin(\omega t + \delta_1) + I_3 \sin(3\omega t + \delta_3) + I_5 \sin(5\omega t + \delta_5) + \ldots . \quad (2)$$

The intensities are normalized by first intensity and the third relative harmonic [$I_{3/1} \equiv I(3\omega)/I(\omega)$, where ω is the excitation frequency] is the most significant intensity among higher harmonics (Hyun *et al.*, 2007; Hyun and Wilhelm, 2009; Hyun *et al.*, 2012).

2.4. Morphology

Field Emission Scanning Electron Microscopy (FE-SEM) observations were carried out using a JSM 6700F microscope at 5 KV to evaluate morphology evolutions. Samples were fractured in liquid nitrogen and then covered with platinum. Locations of C20A were observed by Transmission Electron Microscopy (TEM) using FEI Tecnai G^2 T-20s at an accelerating voltage of 200 KV and room temperature. Samples were cut using a cryo-microtome device at −140°C and put on a copper grid.

3. Result and Discussion

Small amplitude oscillatory shear (SAOS) tests were carried out at 200°C with a fixed strain amplitude of γ_0 = 0.05 within the linear regime. Fig. 1a and 1b shows the complex moduli $G^*(\omega)$ and the complex viscosity $\eta^*(\omega)$ of

the (80/20) PP/PS blend as well as of the virgin polymers PP and PS as a function of frequency and strain amplitudes, respectively. Surprisingly, the modulus and viscosity of the PP/PS blend did not follow the log-additive mixing rule and showed lower values than those of the pure component at all frequencies (see inset plot in Fig. 1a). The storage modulus G'(ω) and loss modulus G"(ω) demonstrated the same trends of the complex modulus G^*(ω) (not shown here). This negative deviation from the log-additive mixing rule (see Fig. 1b) is believed to be due to interfacial slip (Utracki, 1991; Zhao and Macosko, 2002). Since PP and PS have high incompatibility, their corresponding blends show reduction of the complex modulus G^*(ω) due to lower entanglement in their interfacial areas than in the bulk system. Discontinuous shear rate is generated in the low entanglement density area when shear stress is applied. Therefore, a lower modulus is a consequence of slippage at the interface. This lower modulus of the blend was observed in the LAOS test (Fig. 1c). At large deformation ($\gamma_0 > 2.0$), however, the interfacial effect disappeared since the matrix contribution was stronger (see Fig. 1c).

In order to overcome slippage at the interface and improve compatibility between the two phases, compatibilizers were added to the (80/20) PP/PS blend. Introduction of a third component, even a compatibilizer, could have effects depending on the localization of the compatibilizer, *e.g.*, one of the phases or at the interface (Elias *et al.*, 2008; Hong *et al.*, 2008; Zonder *et al.*, 2011). It is also believed that pre-shearing history (processing conditions) could have profound effects on the extent and amplitudes of the linear regime of the modulus (Lertwimolnun and Vergnes, 2006; Cho *et al.*, 2011). Lertwimolnun and Vergnes (2006) found that mixing conditions, feeding rate, and screw speed all have significant effects on rheological properties as well as the degree of exfoliation of PP/C20A composites. They found that the linear dependency of the storage modulus to strain amplitudes decreases with increasing degree of dispersion.

From the SAOS and LAOS tests, the effects of mixing protocol and mixing time on the linear and non-linear rheological properties of PP/PS/C20A blends were investigated. As shown in Fig. 2a and 2b, the linear and non-linear complex moduli G*(ω) of all corresponding PP/PS/C20A blends subjected to four protocols at different time evolutions were plotted. Each protocol was denoted with P, and its numerical index reflects the number of that protocol as described in the previous section. As shown in the results, mixing time did not significantly alter the rheological properties of the P_1 = (PP/PS/C20A simultaneously mixing), P_2 = (PP+C20A/PS), and P_4 = (PP+PS/C20A) blends. However, the complex moduli G*(ω) of the blends mixed for 8 min slightly decreased possibly due to thermal degradation. Interestingly, the

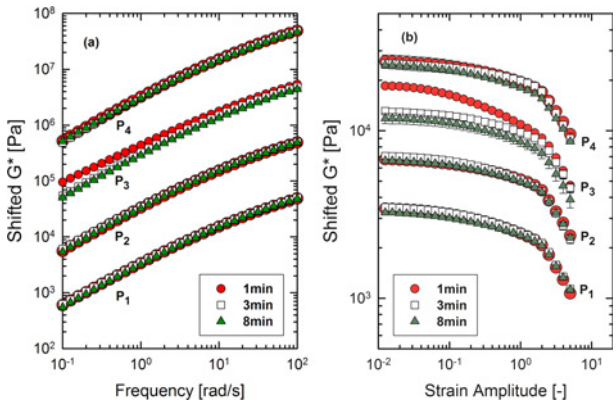

Fig. 2. (Color online) (a) Comparison of linear dynamic rheological properties of PP/PS/C20A blends for all protocols via frequency sweep test at a fixed strain amplitude of 0.05 and a temperature of 200°C. The complex moduli of the P_1=PP/PS/C20A, P_2=PP+C20A/PS, P_3=PS+C20A/PP, and P_4=PP+PS/C20A blends have been artificially shifted by 10^0, 10, 10^2, and 10^3, respectively. (b) Non-linear dynamic rheological properties of PP/PS/C20A blends for all protocols were compared via strain sweep test under LAOS at a fixed frequency of 1 rad/s and a temperature of 200°C. Strain amplitudes varied from 0.01 to 5. Complex moduli of the P_1= PP/PS/C20A, P_2=PP+C20A/PS, P_3=PS+C20A/PP, and P_4= PP+PS/C20A blends have been artificially shifted by 10^0, 2, 4, and 8, respectively, for the sake of clarity.

P_3 = (PS+C20A/PP) blend mixed for 1 min demonstrated much higher G*(ω) values than those mixed for 3 and 8 min for all protocols. Moreover, Fig. 2b shows that the P_3 = (PS+C20A/PP) blend mixed for 1 min exhibited strong non-linear behavior (shear thinning). Indeed, the maximum strain amplitude defining the extent of linearity shifted to lower strain amplitudes in this particular case. It has been reported that this can be attributed to breakdown and re-agglomeration of the filler network when filler interactions are dominant (Cassagnau, 2008; Ramier *et al.*, 2007).

In addition to mixing time, Fig. 3 illustrates the effect of mixing protocol at different times. The P_3 = PS+C20A/PP blend mixed for 1 min showed significant enhancement of the linear complex modulus. This result is similar to that of reported by Ramier *et al.* (2007), who carried out a second strain sweep test 30 min after the first run on silica-reinforced styrene-butadiene rubber (SBR). The silica/SBR sample underwent irreversible breakdown of the filler network. As a result, the elastic modulus G'(γ) of the silica/SBR sample decreased after the second strain sweep run due to permanent network breakdown.

FT-Rheology was used to quantify the non-linear responses of the blends. Fig. 4a and 4b shows the normalized third intensities ($I_{3/1}$) of the blends mixed for 1

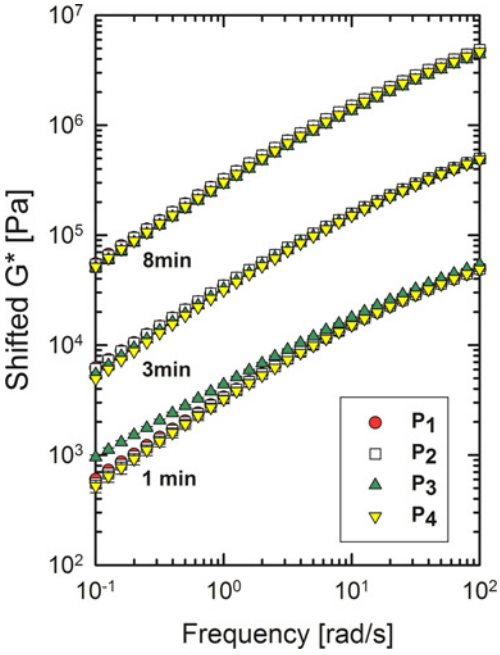

Fig. 3. (Color online) Comparison of the complex moduli of the blends for different protocols at fixed mixing times via frequency sweep tests at a fixed strain amplitude of 0.05 and a temperature of 200°C. Complex moduli of the blends mixed for 1 min, 3 min, and 8 min have been artificially shifted by 10^0, 10, and 10^2, respectively. Different protocols are named as P_1 = PP/PS/C20A, P_2 = PP+C20A/PS, P_3 = PS+C20A/PP, and P_4 = PP+PS/C20A.

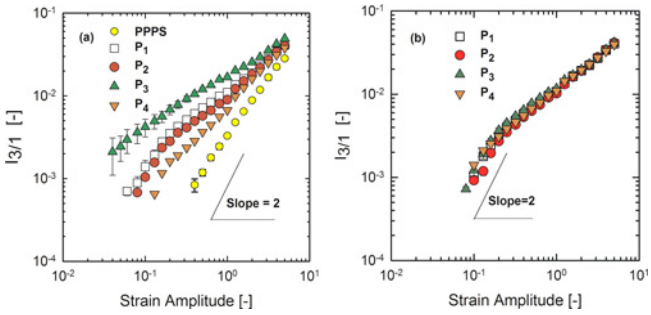

Fig. 4. (Color online) The normalized third relative intensities ($I_{3/1}$) of the P_1 = PP/PS/C20A, P_2 = PP+C20A/PS, P_3 = PS+C20A/PP, and P_4 = PP+PS/C20A blends mixed for (a) 1 min and (b) 8 min as a function of strain amplitude at a fixed frequency of 1 rad/s and a temperature of 200°C.

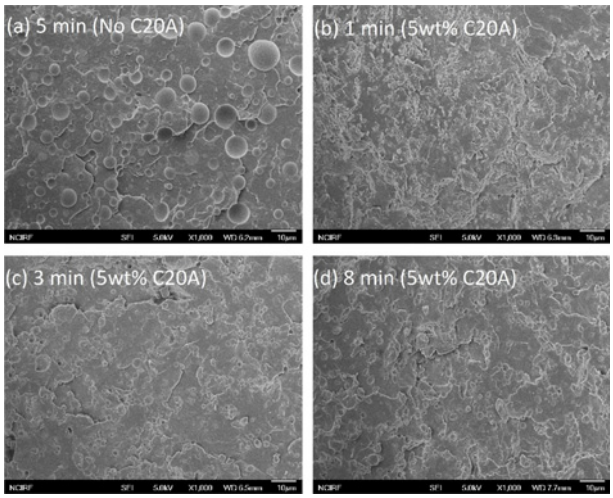

Fig. 5. (Color online) Morphological evolutions of the PP/PS blend mixed for (a) 5 min and P_3 = PS+C20A/PP blends mixed for (b) 1 min, (c) 3 min, and (d) 8 min. Scale bar length is 10 μm. Droplet size of (a) is bigger than (b), (c), and (d).

min and 8 min for all protocols, relatively. The non-linearity ($I_{3/1}$) from FT-Rheology is very sensitive to polymer topology (Hyun and Wilhelm, 2009; Wagner, 2011; Hyun and Kim, 2012; Hyun *et al.*, 2013), microstructure of the polymer blends (Filipe *et al.*, 2004; Salehiyan and Hyun, 2013), and the nanostructure of the polymer composite (Hyun *et al.*, 2012; Lim *et al.*, 2013). Lim *et al.* (2013) concluded that the non-linearity ($I_{3/1}$) is related with interfacial properties of the polymer nanocomposite. Reinheimer *et al.* (2011) reported that the non-linearity ($I_{3/1}$) is related with the inverse of interfacial tension based on a theoretical model for emulsion systems. Compared with the linear rheological properties (Fig. 3) and non-linear rheological properties of 1 min mixing (Fig. 4a), the non-linearity was able to distinguish four different protocols better than the linear rheological properties. Complex modulus G*(ω) (linear rheological properties) represents the modulus for all contributions, i.e., matrix phase (PP), dispersed phase (PS), clay (C20A), and interfacial properties. However, non-linearity can better emphasize contributions of interfacial properties than the properties of PP, PS, or C20A (Lim *et al.*, 2013; Reinheimer *et al.*, 2011). For this reason, Fig. 4a shows very different values of the blends subjected to the different protocols. Especially, P_3 mixed for 1 min showed the largest values compared with the other protocols. Since P_3 mixed for 1 min showed complex morphology (see Figs. 5 and 6), larger non-linearity than the other three protocols was obtained (discussed later). In Fig. 4b, all non-linearity ($I_{3/1}$) at different protocols showed almost the same results. This means that sufficient mixing time (8 min) abrogated the mixing protocol effect (described later).

In polymer nanocomposites, filler interactions with either other adjacent fillers or polymer chains affect the linear and non-linear rheological properties (Cassagnau, 2008). Formation of a three-dimensional interconnected filler network immobilizes polymer chains by entrapping them, thereby increasing the modulus of the polymer

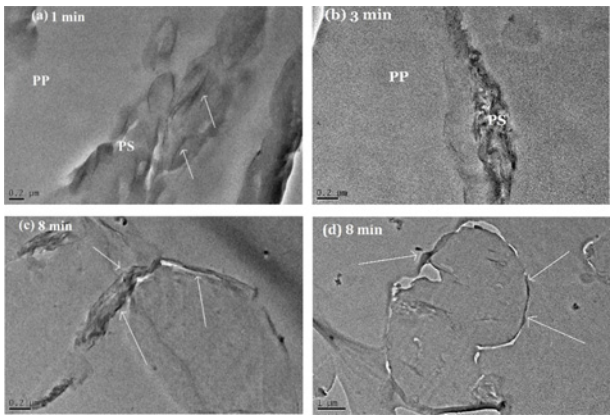

Fig. 6. (Color online) TEM images of the P_3 = PS+C20A/PP blends mixed for (a) 1 min, (b) 3 min, and (c, d) 8 min. Scale bar length is 0.2 μm for (a-c) and 1 μm for (d).

nanocomposite (Cassagnau, 2008; Huitric *et al.*, 2009). Morphological evolution of the blends for this particular protocol reveals interesting results, as shown in Fig. 5.

The SEM images clarify the compatibilization effect of C20A fillers by showing a dramatic reduction in droplet sizes in PP/PS blends (Please compare Fig. 5a and 5b-d). This result is consistence with increase in $I_{3/1}$ values of the PP/PS blend with filler compared without filler (Fig. 4a). Moreover, complex blend morphology (not well-developed morphology) after 1 min of mixing can be seen in Fig. 5b. This unstable morphology could be the reason for the enhancement of rheological properties. Relatively heterogeneous phase after 1 min of mixing compared to 3 min and 8 min of mixing increased non-linearity. Therefore, the rheological properties of the blends mixed for 1 min showed diverse values at each measurement (not shown here; however, the moduli of the blends mixed for 1 min were always larger than those prepared under other conditions). More uniform stress is observed when the morphology is complex and thus the rheological properties enhanced (Li *et al.,* 2007). Shearing for longer times led to formation of droplet morphologies, as observed in Fig. 5. Where morphologies after 3 min and 8 min of mixing showed well dispersed droplets. In fact, clay incorporation increased the viscosity of PS phase, which made it even more difficult for droplets to deform under certain shearing conditions within 1 min of mixing. In the case of P_3 = PS+C20A/PP, clay particles stuck to each other and made particle clusters at lower mixing times (1 min and 3 min). Therefore, clustering of PS phase hosting C20A might induce solid-like behavior at low frequencies (Fig. 3) in the P_3 = PS+C20A/PP blend mixed for 1 min. Furthermore, clay migrations are unlikely within 30 seconds. The migration time could be 30 seconds since the second phase, PP, was added after 30 seconds. The mechanisms of clay migrations are self-diffusion by thermal Brownian motion and external hydrodynamic shear stress with sufficient time (Elias *et al.*, 2008b). Thus, increasing shear time caused the cluster of clay particles to break up into smaller clusters and induced the migration of clays towards the interface. In Fig. 6, TEM images show that clay tactoids remained in PS phase at early stages of mixing. With time, most clays migrated towards the interface where they were thermodynamically more stable. This effect is evident in Fig. 4b in which all relative third intensities ($I_{3/1}$) of the blends mixed for 8 min for this protocol are depicted. In Fig. 4b, all curves showed the same behavior, which indicates that clays reached to the more equilibrium state after 8 min of shearing by migrating towards the interface than that of 1 min and 3 min mixed blends. On one hand, the orientation of these nano-sized clays at the interface of multiphase systems (see Fig. 6c and 6d) can reduce the size of the dispersed phase, as shown in Fig. 5c. On the other hand, localization of the clays at PS phase changes the viscosity of the PS and makes it difficult to deform under shear conditions. Therefore, the P_3 = PS+C20A/PP blend mixed for 1 min did not show any perfect spheres in the dispersed phase due to unwell-deformed parts of PS phase within 30 seconds after addition of PP.

4. Conclusions

Correlation between morphological evolutions and rheological properties of PP/PS/C20A (80/20/5 wt%) blends were studied to determine the effects of mixing protocol and mixing time. It was found that the P_3 = PS+C20A/PP blend mixed for 1 min had the highest values due to its unique complex and not well-mixed morphology which is observed when the dispersed phases is less mixed. TEM images revealed that C20A particles were located inside of PS phase within 1 min. However, the clay particles migrated to the interface where they were more stable upon longer mixing time. It is confirmed that morphology is an important factor affecting rheological properties in this particular blend system (P_3 = PS+C20A/PP). On the other hand, rheological properties of the other blends (P_1, P_2 and P_4) for different protocols with different mixing times were roughly the same. However, viscoelasticities of the blends mixed for 8 min were relatively lower than those of the blends mixed for 1 min and 3 min due to possible thermal degradation. Finally, clay localizations could be a dominant factor to control morphology and viscoelastic properties only within a specific mixing time. Chemical affinity between clays and one of the phases acts as a chemical potential, resulting in the migration of clays from their original locations to the more compatible phase if a certain time is given.

Acknowledgements

This work was supported by a 2-Year Research Grant of Pusan National University and BK21 PLUS Centre for Advanced Chemical Technology (21A20131800002).

References

Asthana, H. and K. Jayaraman, 1999, Rheology of reactively compatibilized polymer blends with varying extent of interfacial reaction, *Macromolecules* **32**, 3412-3419.

Brahimi, B., A. AitKadi, A. Ajji, R. Jérôme, and R. Fayt, 1991, Rheological properties of copolymer modified polyethylene/polystyrene blends, *J. Rheol.* **35**, 1069-1091.

Cassagnau, P., 2008, Melt rheology of organoclay and fumed silica nanocomposites, *Polymer* **49**, 2183-2196.

Cho, S., J.S. Hong, S.J. Lee, K.H. Ahn, J.A. Covas, and J.M. Maia, 2011, Morphology and rheology of polypropylene/polystyrene/clay nanocomposites in batchand continuous melt mixing processes, *Macromol. Mater. Eng.* **296**, 341-348.

Elias, L., F. Fenouillot, J.C. Majeste, and P. Cassagnau, 2007, Morphology and rheology of immiscible polymer blends filled with silica nanoparticles, *Polymer* **48**, 6029-6040.

Elias, L., F. Fenouillot, J.C. Majeste, P. Alcouffe, and P. Cassagnau, 2008, Immiscible polymer blends stabilized with nanosilica particles:Rheology and effective interfacial tension, *Polymer* **49**, 4378-4385.

Elias, L., F. Fenouillot, J.C. Majeste, G. Martin, and P. Cassagnau, 2008, Migration of nanosilica particles in polymer blends, *J. Polym. Sci., Part B: Polym. Phys.* **46**, 1976-1983.

Fayt, R., R. Jerome, and P. Teyssie, 1981, Molecular design of multicomponent polymer systems. I. Emulsifying effect of poly(hydrogenated butadiene-b-styrene) copolymers in LDPE/PS blends, *J. Polym. Sci., Polym. Lett. Ed.* **19**, 79-84.

Filipe, S., M.T. Cidade, M. Wilhelm, and J.M. Maia, 2006, Evolution of the morphological properties along the extruder length for compatibilized blends of a commercial liquid crystalline polymer and polypropylene, *J. Appl. Polym. Sci.* **99**, 347–359.

Gleinser, W., H. Braun, Chr. Friedrich, and H.J. Cantow, 1994, Correlation between rheology and morphology of compatibilized immiscible blends, *Polymer* **35**, 128-135.

Harrats, C., 2010, *Multiphase Polymer-Based Materials: An Atlas of Phase Morphology at the Nano and Micro Scale*, CRC Press.

Hong, J.S., Y.K. Kim, K.H. Ahn, S.J. Lee, and C. Kim, 2007, Interfacial tension reduction in PBT/PE/clay nanocomposite, *Rheol. Acta.* **46**, 469-478.

Hong, J.S., K.Y. Kim, K.H. Ahn, and S.J. Lee, 2008, Shear-induced migration of nanoclay during morphology evolution of PBT/PS blend, *J. App. Polym. Sci.* **108**, 565-575.

Huitric, J., J. Ville, P. Mederic, M. Moan, and T. Aubry, 2009, Rheological, morphological and structural properties of PE/PA/nanoclay ternary blends: Effect of clay weight fraction, *J. Rheol.* **53**, 1101-1119.

Hyun, K., E.S. Baik, K.H. Ahn, S.J. Lee, M. Sugimoto, and K. Koyama, 2007, Fourier-transform rheology under medium amplitude oscillatory shear for linear and branched polymer melts, *J. Rheol.* **51**, 1319-1342.

Hyun, K. and M. Wilhelm, 2009, Establishing a New Mechanical Nonlinear coefficient Q from FT-Rheology: First Investigation on Entangled Linear and Comb Polymer Model Systems, *Macromolecules.* **42**, 411-422.

Hyun, K. and W. Kim, 2011, A new non-linear parameter Q from FT-Rheology under nonlinear dynamic oscillatory shear for polymer melts system, *Korea-Aust. Rheol. J.* **23**, 227-235.

Hyun, K., M. Wilhelm, C.O. Klein, K.S. Cho, J.G. Nam, K.H. Ahn, S.J. Lee, R.H. Ewoldt, and G.H. McKinley, 2011, A Review of nonlinear oscillatory shear tests: analysis and application of large amplitude oscillatory shear (LAOS), *Prog. Polym. Sci.* **36**, 1697-1753.

Hyun, K., H.T. Lim, and K.H. Ahn, 2012, Nonlinear response of polypropylene (PP)/Clay nanocomposites under dynamic oscillatory shear flow, *Korea-Aust. Rheol. J.* **24**, 113-120.

Hyun, K., W. Kim, S.J. Park, and M. Wilhelm, 2013, Numerical simulation results of the nonlinear coefficient Q from FT-Rheology using a single mode pom-pom model, *J. Rheol.* **57**, 1-24.

Iza, M., M. Bousmina, and R. Jerome, 2001, Rheology of compatibilized immiscible viscoelastic polymer blends, *Rheol. Acta.* **40**, 10-22.

Labaume, I., P. Mederic, J. Huitric, and T. Aubry, 2013, Comparative study of interphase viscoelastic properties in polyethylene/polyamide blends compatibilized with clay nanoparticles or with a graft copolymer, *J. Rheol.* **57**, 377-392.

Lertwimolnun, W. and B. Vergnes, 2006, Effect of Processing Conditions on the Formation of Polypropylene/Organoclay Nanocomposites in a Twin Screw Extruder, *Polym. Eng. Sci.* **46**, 314-323.

Li, Y.Y., S.W. Hu, and J. Sheng, 2007, Evolution of phase dimensions and interfacial morphology of polypropylene/polystyrene compatibilized blends during mixing, *Eur. Polym. J.* **43**, 561-572.

Lim, H.T, K.H. Ahn, S.J. Lee, J.S. Hong, and K. Hyun, 2013, Nonlinear viscoelasticity of polymer nanocomposites under large amplitude oscillatory shear flow, *J. Rheol.* **57**, 767-789.

Macaubas, P.H.P., N.R. Demarquette, and J.M. Dealy, 2005, Nonlinear viscoelasticity of PP/PS/SEBS blends, *Rheol. Acta.* **44**, 295-312.

Mederic, P., T. Razafinimaro, T. Aubry, M. Moan, and M.H. Klopffer, 2005, Rheological and structural investigation of layered silicate nanocomposites based on polyamide or polyethylene: influence of processing conditions and volume fraction effects, *Macromol. Symp.* **221**, 75-84.

Raghu, P., C.K. Nere, and R.N. Jagtap, 2003, Effect of styrene–isoprene–styrene, styrene–butadiene– styrene, and styrene–butadiene–rubber on the mechanical, thermal, rheological, and morphological properties of polypropylene/polystyrene blends, *J. Appl. Polym. Sci.* **88**, 266-277.

Ramier, J., C. Gauthier, L. Chazeau, L. Stelandre, and L. Guy, 2007, Payne effect in silica-filled styrene-butadiene rubber: influence of surface treatment, *J. Polym. Sci*, *Polym. Phys.* **45**, 286-298.

Ray, S.S., S. Pouliot, M. Bousmina, and L. A. Utracki, 2004,

Role of organically modifed layered silicate as an active interfacial modifer in immiscible polystyrene/polypropylene blends, *Polymer* **45**, 8403-8413.

Reinheimer, K., M. Grosso, and M. Wilhelm, 2011, Fourier Transform Rheology as a universal non-linear mechanical characterization of droplet size and interfacial tension of dilute monodisperse emulsions, *J. Colloid Interface Sci.* **360**, 818-825.

Salehiyan, R., A.A. Yussuf, N.F. Hanani, A. Hassan, and A. Akbari, Polylactic acid/polycaprolactone nanocomposite: influence of montmorillonite and impact modifier on mechanical, thermal and morphological properties, June, 04, 2013, DOI: 10.1177/0095244313489906, *J. elastomers. plast*.

Salehiyan, R. and K. Hyun, 2013, Effect of organoclay on nonlinear rheological properties of poly(lactic acid)/poly(caprolactone) blends, *Korean J. Chem. Eng.* **30**, 1013-1022.

Utracki, L. A., 1991, On the viscosityconcentration dependence of immiscible polymer blends, *J. Rheol.* **35**, 1615-1637.

Utracki, L. A and P. SAMMUT, 1988, Rheological Evaluation of Polystyrene/Polyethylene Blends, *Polym. Eng. Sci.* **28**, 1405-1415.

Van Hemelrijck, E., P. Van Puyvelde, S. Velankar, C.W. Macosko, and P. Moldenaers, 2003, Interfacial elasticity and coalescence suppression in compatibilized polymer blends, *J. Rheol.* **48**, 143-158.

Van Hemelrijck, E., P. van Puyvelde, and P. Moldenaers, 2006, Rheology and morphology of highly compatibilized polymer blends, *Macromol. Symp.* **233**, 51-58.

Van Puyvelde, P., S. Velankar and P. Moldenaers, 2001, Rheology and morphology of compatibilized polymer blends, *Curr. Opin. Colloid Interface Sci.* **6**, 457-463.

Vermant, J., G. Cioccolo, K. Golapan Nair, and P. Moldenaers, 2004, Coalescence suppression in model immiscible polymer blends by nano-sized colloidal particles, *Rheol. Acta.* **43**, 529-538.

Wagner, M.H., V.H. Rolón-Garrido, K. Hyun, and M. Wilhelm, 2011, Analysis of medium amplitude oscillatory shear (MAOS) data of entangled linear and model comb polymers, *J.Rheol.* **55**, 495-516.

Wang, Y., Q. Zhang, and Q. Fu, 2003, Compatibilization of immiscible poly(propylene)/polystyrene blends using clay, *Macromol. Rapid Commun.* **24**, 231-235.

Wilhelm, W., D. Maring, and H.W. Spiess, 1998, Fourier-transform rheology, *Rheol. Acta.* **37**, 399-405.

Wilhelm, W., P. Reinheimer, and M. Ortseifer, 1999, High sensitivity Fourier-transform rheology, *Rheol. Acta.* **38**, 349-356.

Wilhelm, W., P. Reinheimer, M. Ortseifer, T. Neidhofer, and H.W. Spiess, 2000, The crossover between linear and non-linear mechanical behaviour in polymer solutions as detected by Fourier-transform rheology, *Rheol. Acta.* **39**, 241-246.

Zhao, R and C.W. Macosko, 2002, Slip at polymer–polymer interfaces: Rheological measurements on coextruded multilayers, *J. Rheol.* **46**, 145-167.

Zonder, L., A. Ophir, S. Kenig, and S. McCarthy, 2011, The effect of carbon nanotubes on the rheology and electrical resistivity of polyamide 12/high density polyethylene blends, *Polymer* **52**, 5085-5091.